Effective bilayer expansion and erythrocyte shape change induced by monopalmitoyl phosphatidylcholine

Quantitative light microscopy and nuclear magnetic resonance spectroscopy measurements

Lang-Ming Chi and Wen-guey Wu
Institute of Life Sciences, National Tsing Hua University, Hsinchu, Taiwan 30043 Republic of China

ABSTRACT When human erythrocytes are treated with exogenous monopalmitoyl phosphatidylcholine (MPPC), the normal biconcave disk shape red blood cells (RBC) become spiculate echinocytes. The present study examines the quantitative aspect of the relationship between effective bilayer expansion and erythrocyte shape change by a newly developed method. This method is based on the combination of direct surface area measurement of micropipette and relative bilayer expansion measurement of ^{13}C cross-polarization/magic angle spinning nuclear magnetic resonance (NMR). Assuming that ^{13}C NMR chemical shift of fatty acyl chain can be used as an indicator of lateral packing of membrane bilayers, it is possible for us to estimate the surface area expansion of red cell membrane induced by MPPC from that induced by ethanol. Partitions of lipid molecules into cell membrane were determined by studies of shape change potency as a function of MPPC and red cell concentration. It is found that $8(\pm 0.5) \times 10^6$ molecules of MPPC per cell will effectively induce stage three echinocytes and yield $3.2(\pm 0.2)\%$ expansion of outer monolayer surface area. Surface area of normal cells determined by direct measurements from fixed geometry of red cells aspirated by micropipette was $118.7 \pm 8.5\ \mu m^2$. The effective cross-sectional area of MPPC molecules in the cell membrane therefore was determined to be $48(\pm 4)\ Å^2$, which is in agreement with those determined by x-ray from model membranes and crystals of lysophospholipids. We concluded that surface area expansion of RBC can be explained by a simple consideration of cross-sectional area of added molecules and that erythrocyte shape changes correspond quantitatively to the incorporated lipid molecules.

INTRODUCTION

Sheetz and Singer (1) first proposed that amphipathic drugs induce morphologic changes of human red blood cells (RBC)[1] by the mechanism of "bilayer couple hypothesis" (1). On the basis of this model, the shape of RBC could change from the normal biconcave disk shape to either echinocytes or stomatocytes depending on the balance of the surface area for the two monolayers in the membrane. For the past 15 yr, this hypothesis has been supported by numerous studies (2–7) and successfully predicted the effect of many others (8–16).

The sensitivity of the aforementioned shape-controlling mechanism has long been appreciated. It has been noted that <1% increase in the area ratio can account for the profound change in the morphology of the cell (1, 3). Previous assessment relied mainly on the detection of amphipathic concentrations occupied by the two monolayers. Fluorescence probe (6), radioactive labeling (7, 8), and spin-labeled compounds (4, 7) have been used to measure the quantitative aspects of this hypothesis. By assuming the cross-sectional areas of these molecules in red cell membranes, the expansion of the outer monolayer (or contraction of the inner monolayer) were determined to be in the range of 1–5% depending on stages of shape changes. Interestingly, calculations of the inner and outer surface areas by using geometrical models of echinocyte spikes yield an estimated value of 0.4–0.9% (7), which is smaller.

The present study was designed to determine the minute bilayer expansion of the erythrocytes membranes by the combination of light microscopy and nuclear magnetic resonance (NMR) spectroscopy measurements. First, we used light microscope and micropipette aspiration for direct surface area measurements of RBC with or without monopalmitoyl phosphatidylcholine (MPPC) or ethanol. Because levels of lipid incorporation into cell membranes are not high enough to cause measurable surface area expansion by micropipette technique, we perform ^{13}C-NMR measurements to relate bilayer expansion of RBC treated with ethanol with those treated with MPPC. Finally, concentrations of MPPC incorporated into RBC membranes were determined by the variation of shape changes potency with MPPC and red cell concentrations. Our data show comparable results with those

[1] *Abbreviations used in this paper:* CP/MAS, cross-polarization/magic angle spinning; Kp, partition coefficient; MI, morphological index; MPPC, monopalmitoylphosphatidylcholine; NMR, nuclear magnetic resonance; RBC, red blood cell; TMS, tetramethylsilane.

0006-3495/90/06/1225/08 $2.00

obtained previously by other methods and the effective cross-sectional area of MPPC to induce membrane expansion was determined to be 48 ± 4 Å^2.

MATERIALS AND METHODS

Materials

MPPC was purchased from Sigma Chemical Co. (St. Louis, MO). Ethanol and other chemicals were purchased from Merck (Rahway, NJ) with reagent grade.

Blood was obtained from healthy adult volunteers by venipuncture and collected into 3.2% sodium citrate, blood/sodium citrate = 9:1 (vol/vol). RBC were separated from plasma and buffy coat by centrifugation at 3,000 *g* for 5 min (International Equipment Co. Centra-4B, San Francisco, CA). Erythrocytes were washed three times with 4 vol of 150 mM NaCl and once with 138 mM NaCl, 5 mM KCl, 6.1 mM Na_2HPO_4, 1.4 mM NaH_2PO_4, 1 mM $MgSO_4$, 5 mM glucose, pH 7.4 (NaCl/Pi) (4) or 150 mM NaCl, 0.25% BSA, 0.1% EDTA, pH 7.4 (BSA-Tris buffer) (for micropipette experiments only) (17). After removal of the supernatant, the packed erythrocytes were suspended with NaCl/Pi, or BSA-Tris buffer to proper hematocrit, and incubated with reagents at room temperature for ~2–3 h.

Morphology assay

Erythrocytes, 0.01, 0.2, 2, and 50% hematocrit, were incubated with different concentrations of MPPC at room temperature (21–23°C) for 3 h. Within this period, one drop (~30 μl) of cell was withdrawn at specified time intervals then prepared for morphological assay.

Erythrocytes were fixed with hematocrit below 5% in 0.5% glutaraldehyde in 150 mM NaCl for at least 20 min to stop shape change process and preclude the "glass effect." Cells were then moisturized in 40% glycerol and viewed by 1000× phase-contrast microscope. Cell morphology was graded on a scale of (+1)–(+5) for echinocyte and (−1)–(−4) for stomatocyte based on the nomenclature of Bessis (18). The average score of 100 erythrocytes in several fields was taken as the morphological index (MI).

Cross-polarization/magic angle spinning (CP/MAS) ^{13}C-NMR experiments

Unsealed RBC ghost membranes were prepared by lyzing the well-washed cells with 5 mM sodium phosphate, pH 8.0 (5P8), and centrifuged at 22,000 *g* for 10 min (19). The pellet was washed with the same buffer until it was white. The packed white unsealed ghost was condensed by centrifugation at 3 × 10^5 *g* for ~5–6 h. The lowest pellet with yellow membrane was collected and weighed. Known amounts of either MPPC or ethanol were then added to the packed ghost membrane in the spinner to a total volume of 300 μl. After 1 h incubation and stirring by vortex at room temperature, the spinner was then used for CP/MAS ^{13}C-NMR detection. The protein concentrations were assayed by lowry method (20), and 0–0.2 mg/ml of bovine serum albumin (BSA) were used as standard and ghost membrane concentrations were estimated by protein content (assuming 5.7 × 10^{-10} mg of membrane protein per ghost). Concentrations of added amphipaths (number of either MPPC or ethanol molecules per ghost) were calculated according to Eq. 3 (see below) by the known partition coefficient (21), total volume, and ghost membrane concentration.

The ^{13}C spectra of ghost membrane were obtained at room temperature by combination of CP/MAS approach (22, 23) and proton decoupling and performed on a NMR spectrometer (model MSL-200; Bruker Instruments, Inc., Billerica, MA) in conjunction with an Andrew type MAS probe. The spinner was made of ZrO_2 or Al_2O_3 with an internal volume of 350 μl and was spun with compressed air at 1.5 KHz. Adamantane was utilized to match the "Hartman–Hahn" condition, and to determine the 90° pulse of ^{1}H and ^{13}C. Under these conditions the H_1 fields for ^{1}H and ^{13}C were 200.13 and 50.33 MHz, respectively. Contact times were typically 2 ms. The chemical shift scale was relative to tetramethylsilane (Me_4Si; TMS). Peak assignment was according to Oldfield et al. (24). Because the resonances arising from ^{13}C of phosphocholine do not show any appreciable shift upon addition of ethanol or MPPC, these peaks were used as internal references for the determination of the relative change of hydrocarbon chain signals.

Measurement of the surface area of RBC

0.01% hematocrit of RBCs were suspended in BSA–Tris buffer and transferred to a hand-made chamber mounted on inverted phase-contrast microscope (17). Amplifying 5,000-folds on video monitor, the surface area of one cell was measured by micropipettes with radii of ~0.5–0.8 μm as shown in Fig. 3. By aspiration of the cell it formed a sphere outside the micropipette and a cylinder with a hemispheric cap inside the micropipette. The surface area of cell was quantified as follows:

$$S = 4\pi r_0^2 + 2\pi r_p l + \pi r_p^2, \quad (1)$$

where S is the surface area of cell, r_0 and r_p are the radius of the sphere outside the micropipette and of the micropipette, respectively, and l is the length of the cylindrical part of cell in the micropipette. The surface area parameters, given as mean ±SD values, are the average of 15–22 cells at each MPPC or ethanol concentrations. Surface area of cells treated with MPPC or ethanol were normalized to the control cells on the same day. Because BSA is known to effect the MPPC uptake of RBC (3), but is not dispensable in the micropipette measurements, we have made concentration correction according to the shape change curves with and without BSA.

Estimation of MPPC uptake by hematocrit dependence of shape changes

It is reasonable to assume that to achieve some degree of morphological shape changes, there must be a certain critical concentration of MPPC in the membranes (N_m/V_m). We can then write

$$V_b/V_m = [K_p/(N_m/V_m)](N_t/V_m) - Kp, \quad (2)$$

where $C_m = N_m/V_m$. V_t, V_b, and V_m are the total, buffer, and membrane volume, respectively, and $V_t \simeq V_b + V_m$. By plotting the V_b/V_m against the N_t/V_m values, one can estimate partition coefficient (K_p) from the y-intercept and N_m/V_m from the inverse of the slope (25). Once the partition coefficient is known, one may use the following equation to calculate the concentration in the membranes (C_m)

$$C_m = \frac{C_{aq} \times V_t \times Kp}{V_b + V_m \times Kp}, \quad (3)$$

where C_{aq} is the initial amphipathic concentration in aqueous solution. The following numerical values were used for calculation throughout the experiments when necessary: 5.2 × 10^{-13} g lipid per ghost; 5.7 × 10^{-13} g

protein per ghost; 10^{10} cells per ml packed RBC; 6×10^9 ghost cells per ml, $Kp_{(ethanol)} = 0.14$; $Kp_{(MPPC)} = 7.25 \times 10^4$ (25–27 and this study).

RESULTS

RBC shape changes as a function of hematocrit

Erythrocytes were incubated with various concentrations of MPPC, and their morphological changes were assessed by light microscope. Series of such incubation at indicated hematocrit are shown in Fig. 1. As it has been reported previously, the addition of MPPC will induce crenation; and, the degree of crenation depends on the amount of exogenous lipids. The amount of MPPC needed to induce a certain stage of shape increased with the hematocrit, indicating the partition behavior of the amphipath. The average Kp ($=7.25 \pm [0.03] \times 10^4$) was determined by plotting the volume ratio of buffer to membrane (V_b/V_m) vs. the total amount of MPPC per membrane volume required to induce a certain stage of echinocytes (Fig. 2; also see Eq. 2). Substituting this value into Eq. 3, we found that uptake of $8.0(\pm 0.5) \times 10^6$ MPPC per cell is required to induce stage three echinocytes. This result is in remarkable agreement with a previously determined value, i.e., 7×10^6 lysoPC molecules per cell, based on binding measurements (7).

Surface area of RBC measured by micropipette

We estimated the surface area expansion of the RBC induced by the added amphipath on inverted phase-contrast microscope. Shown in Fig. 3 *A* is the illustrated shape of RBC after aspiration by 0.5 μm diam micropipette. Simple geometry consideration allows us to calcu-

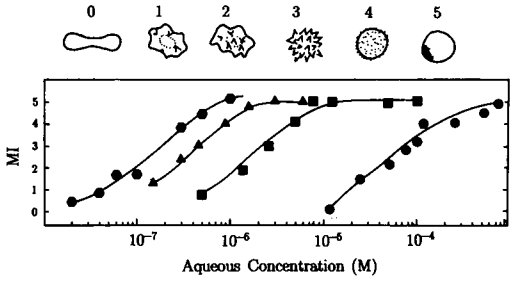

FIGURE 1 RBC shape changes as a function of MPPC and red cell concentration. Cells of 0.01%(●), 0.2%(▲), 2%(■), and 50%(●) hematocrits were incubated with known concentration of MPPC solution and 30 μl of cell was withdrawn at 5, 15, 30, 60, 120, and 180 min intervals to prepare for morphological assay. RBC shape shows no variation between 15 min and 3 h. The MI was the average score of cell shape as indicated on the top of the figure.

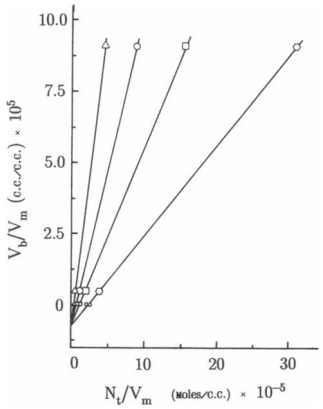

FIGURE 2 Determination of the partition coefficient of MPPC into red cells by shape changes. From the data in Fig. 1, the total MPPC in the solution/total membrane volume (N_t/V_m) which causes stage 1(△), 2(○), 3(□), and 4(◯) echinocytes in 60 min was determined by interpolation and plotted against the corresponding volume ratio of buffer to membranes (V_b/V_m) according to Eq. 2. From the y-intercept, $Kp = 7.25\ (\pm 0.03) \times 10^4$. From the slope, we calculate the stage 1, 2, 3, and 4 echinocytes in 60 min were caused by 2.4×10^6, 4.3×10^6, 8×10^6, and 1.6×10^7 molecules of bound MPPC/cell, respectively.

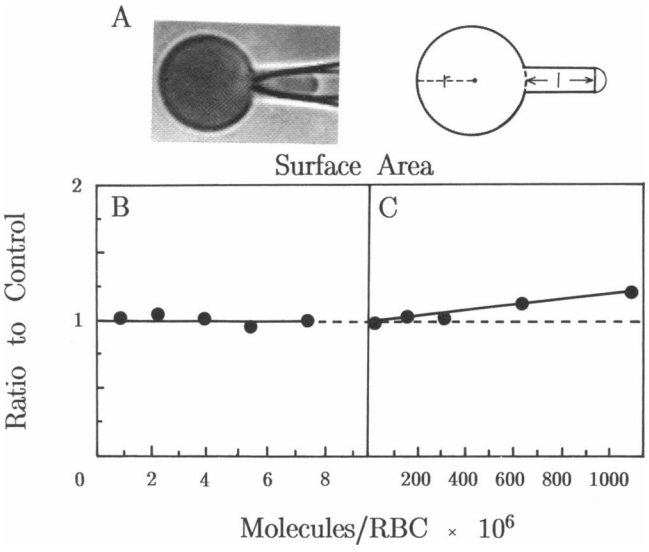

FIGURE 3 Determination of surface area of RBC by micropipette aspiration (*A*) geometry of RBC after aspiration, (*B*) percentage change of surface area expansion of RBC at indicated concentration of MPPC, or (*C*) ethanol. Under aspiration, the red cell formed a measurable model consisting of a sphere outside the micropipette and a cylinder with a hemispheric cap inside the micropipette. The surface area of RBC was calculated from Eq. 1. 0.01% hematocrit of RBCs were suspended in BSA–Tris buffer. Each data point consists of ~20 pairs of cells. The surface area was expressed as the ratio of the value for the MPPC or ethanol treated cells to the value for the control cells ($118.7 \pm 8.7\ \mu^2$). Concentration of MPPC in RBC have been calibrated according to the shape change curves in the presence and absence of BSA.

late the surface area of RBC and the area expansion induced by the incorporation of added molecules. Fig. 3, *B* and *C*, show the measured results for MPPC and ethanol, respectively. It can be seen that, in the studied concentration range, ethanol increases the cell surface area linearly to as much as 20 ± 2% ($n \simeq 20$ for each data point) at 1.2 M bulk ethanol concentration (or 1.1×10^9 molecules per RBC). Control cells show a standard surface area of normal cells with values of 118.7 ± 8.5 μm^2 ($n = 100$). The levels of MPPC incorporation into cell membranes, however, are not high enough to cause any measurable surface expansion (Fig. 3 *B*). Micropipette studies on higher concentration of lipid incorporation are not possible due to the extensive vesiculation of RBC (28).

Relative bilayer expansion measured by NMR

^{13}C CP/MAS NMR measurements were performed on the condensed erythrocyte ghost membrane. As shown in Fig. 4 *A*, most of the peaks come from carbons of lipid molecules. The arrow indicates signal arising from polymethylene hydrocarbon chain, which will be used as an indicator of surface area expansion of RBC. Fig. 4 *B* summarizes the results of ^{13}C–NMR chemical shift of this hydrocarbon chain signal as functions of ethanol and MPPC concentrations. Concentrations of MPPC and ethanol in ghost membranes were determined according to Eq. 3 by using known parameters described in Materials and Methods. It indicates that, at a studied concentra-

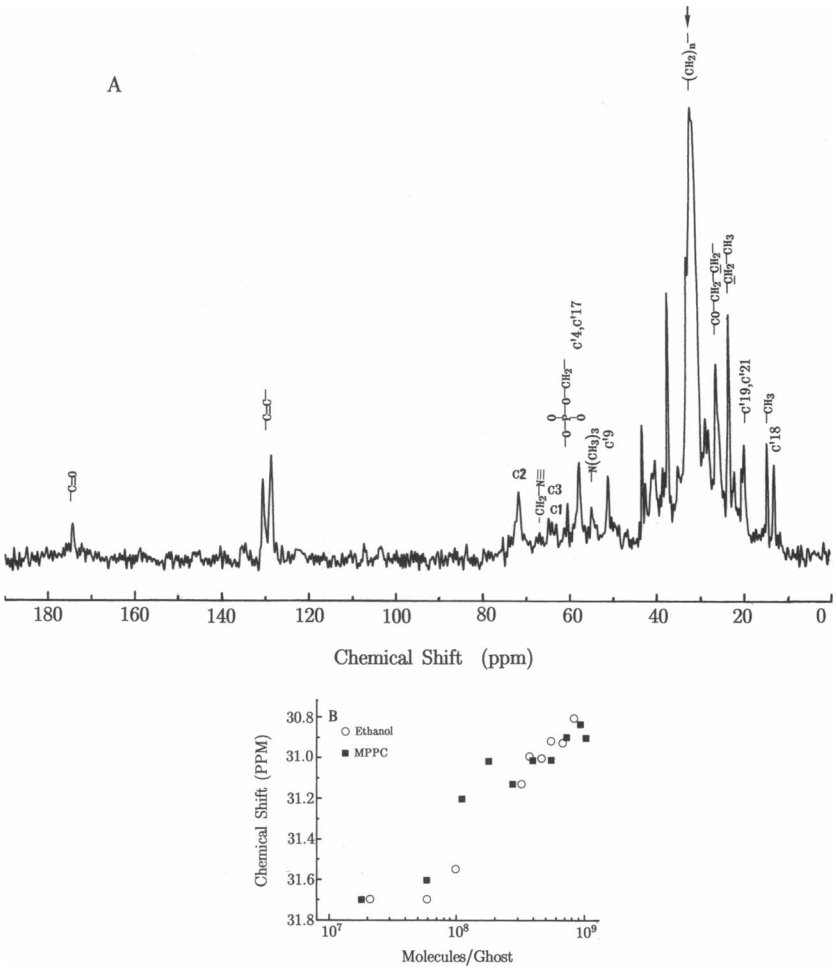

FIGURE 4 (*A*) CP/MAS ^{13}C–NMR spectrum obtained from packed ghost membranes, and (*B*) effect of MPPC or ethanol molecules on the chemical shift of fatty acid hydrocarbon chain resonance. ^{13}C–NMR experiments were conducted in 3 h at 50.33 MHz at room temperature. The relaxation delay was 1.5 s and contact time was 2 ms. Chemical shifts were relative to TMS.

tion range, ^{13}C chemical shift will shift upfield by the addition of exogenous MPPC or ethanol. Within experimental errors, the effective concentrations for MPPC and ethanol to induce changes of ^{13}C chemical shift are similar. Assuming that ^{13}C–NMR chemical shift of fatty acyl chain can be used as an indicator of lateral packing of membrane bilayers (see Discussion), we can estimate surface area expansion induced by MPPC from those induced by ethanol (Fig. 3 *C*).

Effective bilayer expansion and erythrocyte shape

As shown in Fig. 5, the erythrocyte shape change induced by adding MPPC can be correlated with the percentage increase of surface area. Data points were calculated from results of Fig. 1 by using the obtained partition coefficient. The percentage of surface area expansion of MPPC-treated RBC was extrapolated from that of ethanol-treated cells (Fig. 3 *C*) according to Fig. 4. For stage three echinocyte, the outer monolayer surface area expansion was found to be at 3.2% for MPPC. Because the total amount of MPPC per cell required to induce stage three echinocyte has been determined to be 8×10^6, using the determined surface area of RBC, the effective bilayer expansion induced by one molecule of MPPC becomes 48 ± 4 Å^2.

DISCUSSION

Several previous studies have estimated the amount of outer monolayer expansion needed to induce crenation (3, 7, 8). The only available experimental method so far is by using the data of amphipath binding and the assumed cross-sectional surface area of the molecules. Results obtained by this method are usually much higher (3, 6, 7), sometimes up to one order of magnitude, than those estimated by the geometrical models consideration of echinocyte spikes. It is thus important for us to resolve this discrepancy by an independent method.

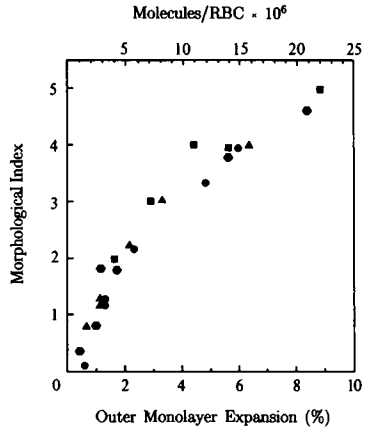

FIGURE 5 Morphological index of RBC plotted as a function of monolayer surface area expansion and MPPC molecules partition in each cell. See text for details.

The most direct measurements to monitor the expansion of surface area of RBC would be the light microscopic method. Due to the unknown geometry of biconcave or spiculate erythrocyte, one has to induce its shape into fixed geometry. This can be done by adding water to swell cell into a sphere. The surface area of normal RBC measured by the swelling method was in the range of ~130–138 μm^2 (29), which is almost 20% higher than our determined value, i.e., 118.7 ± 8.5 μm^2. The reason for the difference between these two results is not clear. One possible explanation is that the micropipette method would be an underestimation due to the folding of membrane during aspiration process and the swelling method would be an overestimation due to the expansion of membrane caused by osmotic pressure effect. However, the above mentioned drawback should not effect the conclusion drawn in the present study. Only a small portion of cell membranes was aspirated into the micropipette, as shown in Fig. 3 *A*. Therefore, it will only change the determined surface area slightly if there is any membrane folding caused by aspiration.

We were not successful in estimating the minute expansion of MPPC-treated RBC by using light microscopic method. There are two main reasons for the failures. First, at higher concentration of MPPC, fragmentation of red cell membrane will occur due to extensive vesiculation (28, 30). Second, the extent of surface area expansion of RBC at low concentration of MPPC would be too small to be outside the experimental error (typically 10% SD). Fortunately, ethanol could induce expansion of surface area to a measurable amount without fragmentation of cell membranes. By correlating results of micropipette and NMR, it is possible to estimate the amount of surface area expansion for certain stages of RBC shape induced by MPPC.

It should be noted that the validation of the present technique is based on the assumption that we can extrapolate surface area data from ethanol to those of MPPC. There are two main points needed to be considered before one makes such an extrapolation. First, lysolecithin is known to locate only in the outer leaflet of cell membranes (31), whereas ethanols penetrate through membranes and are present in both sides of bilayers (32). For this reason, there should be evidence of two populations of NMR data in MPPC experiments. Unfortunately, due to

the linewidth of hydrocarbon chain signals (~3 ppm), it is not possible for us to resolve two peaks with 1-ppm chemical shift difference. There are, however, detectable shoulders for hydrocarbon chain signals by the addition of MPPC (data not shown). In contrast, ^{13}C–NMR linewidth decreases slightly in the presence of ethanol. These results suggest that, similar to intact RBC (3, 4), lysolecithin remains in the outer monolayer even in the ghost membranes. One should thus take this into consideration when performing an estimation of MPPC uptake by RBC. Second, the interaction of ethanol with RBC membranes might be different from those of MPPC. As a consequence, it is by no means obvious that both ethanol and MPPC can induce the same amount of upfield shift of the chemical shift to represent their relative surface area. This is especially true if these two molecules could also interact with membrane proteins (30, 33). At the present time we are not able to exclude the possibility that membrane protein could also play a role in changing the biophysical properties of RBC treated with different amphipaths. However, unpublished results in this laboratory show that both the ethanol- and MPPC-induced hemolysis and morphological changes of RBC depend very much on the partition behavior of these two molecules. It indicates that membrane lipid bilayers serve as a major target for the interaction of these two molecules. One could then directly extrapolate results obtained from ethanol to those of MPPC.

The data presented in Fig. 5 show that 8×10^6 molecules of MPPC incorporation into RBC yield 3.2% expansion and corresponds to stage three morphology. Our experimental estimates agree well with previous lipid binding data and the experimental measured surface area expansion (3, 7). It should be pointed out that our determination of the uptake of MPPC into RBC membranes does not necessarily exclude the cell-associated MPPC. The consistency of our data with previous spin-labeling and radiolabeling results (7), however, suggest that cell-associated lipid micells, if they exist, must be small. Any appreciable cell-associated lipid micells would reduce the amount of lipid incorporation into bilayer membranes. It would then result in an overestimation of an effective cross-sectional area of MPPC. Thus, the RBC concentration dependent behavior of RBC shape change suggested strongly that the intercalation of lipid molecules into the membrane is the main factor for the shape change.

Using our determined surface area of normal RBC, i.e., 119 μm^2, we calculated the cross-sectional area of MPPC molecules in the red cell membrane to be 48 Å^2. It has been shown that the surface area available to one lysolecithin molecule and one cholesterol molecule in hydrated lamellar structures varies from 60–85 Å^2 (34). Assuming that the cholesterol molecule has a fixed area of ~39 Å^2, the area occupied by lysolecithin is between 21 and 46 Å^2 (3). The area of lysophospholipid analogue occupied in the layer surface has also been determined from crystals (35) and interdigitated bilayers (36). The average area per molecule at the lipid/water interface for fully hydrated interdigitated bilayer and crystals were found to be 45.5 Å^2 and 52 Å^2, respectively. Our measurement is consistent with those obtained by x-ray method. This is somewhat surprising if one considers that the areas determined by x-ray method are actually a combination of lysophospholipid and the other "supporting" molecules, such as cholesterol or lysophospholipid itself. One possible explanation for the apparent consistency of the results would be that the space of ~45 Å^2 is required for lysophosphatidylcholine to become stable in the bilayer no matter whether it is located in the model systems or in the biological membranes.

Finally, comment should be made on the usage of ^{13}C–NMR technique to monitor the relative bilayer expansion (37). The main resonance at 31 ppm relative to TMS originates from fatty acyl hydrocarbon chain of membrane lipids. ^{13}C–NMR chemical shift of hydrocarbon chain is due to the *gauche* effect (38). High population of *gauche* conformation in comparison to *trans* would indicate a fluid phase (39), and cause NMR chemical shifts to move to the upfield. This is the case we observed in the present study of MPPC and ethanol effects. The ^{13}C spectra of synthetic model membranes has also been obtained and it shows that the melting of dipalmitoyl phosphatidylcholine dispersions will move the chemical shift of ^{13}C signals of hydrocarbon chains upfield by 2 ppm (data will be published elsewhere). Because the average surface area of lipid molecules in gel and liquid states are 50 Å^2 and 60 Å^2, respectively, it suggests that our ^{13}C–NMR results reflect changes of lipid lateral packing. The advantage of NMR in monitoring these phenomena is that the "absolutely" value detected for the chemical shift is an indicator for both *trans-gauche* isomerization and lateral packing. Thus, to a first-order approximation, we could directly relate the value of chemical shift to surface area expansion. The consistency of our measured results with those determined by x-ray method justifies itself for the applicability of presently developed methods.

In conclusion, a new method based on quantitative micropipette aspiration and NMR measurements have been performed to estimate the surface area expansion of RBC at several stages of shape changes induced by MPPC. The amount of surface area expansion is found to be a result of a simple additive effect of the cross-sectional area of incorporated lipid molecules.

We thank professor Shu Chien for the usage of micropipette aspiration apparatus in the Institute of Biomedical Science, Academic Sinica,

Taiwan. Thanks also to professor Cheng-Teh Wang and Dr. Chung Wang for commenting on the manusript and the encouragement during the process of this work.

This investigation was supported by the National Science Council, R.O.C., under grants NSC-76-0208-M007-82 and NSC-77-0208-M007-92. Ms. Chi was a recipient of a predoctoral fellowship from National Science Council.

Received for publication 30 October 1989 and in final form 26 January 1990.

REFERENCES

1. Sheetz, M. P., and S. J. Singer. 1974. Biological membranes as bilayer couples. A molecular mechanism of drug-erythrocyte interactions. *Proc. Natl. Acad. Sci. USA.* 71:4457–4461.
2. Sheetz, M. P., R. G. Painter, and S. J. Singer. 1976. Biological membranes as bilayer couples. III. Compensatory shape changes induced in membranes. *J. Cell Biol.* 70:193–203.
3. Lange, Y., and J. M. Slayton. 1982. Interaction of cholesterol and lysophosphatidylcholine in determining red cell shape. *J. Lipid Res.* 23:1121–1127.
4. Seigneuret, M., and P. F. Devaux. 1984. ATP-dependent asymmetric distribution of spin-labeled phospholipids in erythrocyte membrane: relation to shape changes. *Proc. Natl. Acad. Sci. USA.* 81:3751–3755.
5. Isomaa, B., H. Hägerstrand, and G. Paatero. 1987. Shape transformations induced by amphiphiles in erythrocytes. *Biochim. Biophys. Acta.* 899:93–103.
6. Matayoshi, E. D. 1980. Distribution of shape-changing compounds across the red cell membrane. *Biochemistry.* 19:3414–3422.
7. Ferrell, J. E., K.-J. Lee, and W. H. Huestis. 1985. Membrane bilayer balance and erythrocyte shape: a quantitative assessment. *Biochemistry.* 24:2849–2857.
8. Ferrell, J. E., and W. H. Huestis. 1984. Phosphoinositide metabolism and the morphology of human erythrocytes. *J. Cell Biol.* 98:1992–1998.
9. Daleke, D. L., and W. H. Huestis. 1985. Incorporation and translocation of aminophospholipids in human erythrocytes. *Biochemistry.* 24:5406–5416.
10. Seigneuret, M., A. Zachowski, A. Hermann, and P. F. Devaux. 1984. Asymmetric lipid fluidity in human erythocyte membrane: new spin-label evidence. *Biochemistry.* 23:4271–4275.
11. Bergmann, W. L., V. Dressler, C. W. M. Haest, and B. Deuticke. 1984. Reorientation rates and asymmetry of distribution of lysophospholipids between the inner and outer leaflet of the erythrocyte membranes. *Biochim. Biophys. Acta.* 772:328–336.
12. Connor, J., and A. J. Schroit. 1988. Transbilayer movement of phosphatidylserine in erythrocytes: inhibition of transport and preferential labeling of a 31000-dalton protein by sulfhydryl reactive reagents. *Biochemistry.* 27:848–851.
13. Middelkoop, E., E. E. Van der Hock, E. M. Bevers, P. Comfurius, A. J. Slotboom, J. A. F. Op den Kamp, B. H. Lubin, R. F. A. Zwaal, and B. Roelofsen. 1989. Involvement of ATP-dependent aminophospholipid translocation in maintaining phospholipid asymmetry in diamide-treated human erythrocytes. *Biochim. Biophys. Acta.* 981:151–160.
14. Sune, A., P. Bette-Bobillo, A. Bienvenue, P. Fellmann, and P. F. Devaux. 1987. Selective outside-inside translocation of aminophospholipids in human platelets. *Biochemistry.* 26:2972–2978.
15. Bevers, E. M., R. H. J. Tilly, J. M. G. Senden, P. Comfurius, and R. F. A. Zwall. 1989. Exposure of endogenous phosphatidylserine at the outer surface of stimulated platelets is reversed by restoration of aminophospholipid translocase activity. *Biochemistry.* 28:2382–2387.
16. Williamson, P., R. Antia, and R. A. Schlegel. 1987. Maintenance of membrane phospholipid asymmetry: lipid-cytoskeletal interactions or lipid pump? *FEBS (Fed. Eur. Biochem. Soc.) Lett.* 219:316–320.
17. Chien, S., K.-L. P. Sung, R. Skalak, S. Usami, and A. Tözeren. 1978. Theoretical and experimental studies on viscoelastic properties of erythrocyte membrane. *Biophys. J.* 24:463–487.
18. Bessis, M. 1973. Red cell shapes: an illustrated classification and its rationale. *In* Red Cell Shape. M. Bessis, R. I. Weed, and P. F. Leblond, editors. Springer-Verlag, New York. 1–24.
19. Hanahan, D. J., and J. E. Ekholm. 1974. The preparation of red cell ghosts (biomembranes). *Methods Enzymol.* 31:168–180.
20. Lowry, O. H., N. J. Rosebrough, A. L. Farr, and R. J. Randall. 1951. Protein measurement with the Folin phenol reagent. *J. Biol. Chem.* 193:265–275.
21. Seeman, P., S. Roth, and H. Schneider. 1971. The membrane concentrations of alcohol anesthetics. *Biochim. Biophys. Acta.* 225:171–184.
22. Maciel, G. E. 1984. High-resolution nuclear magnetic resonance of solids. *Science (Wash. DC).* 226:282–288.
23. Ackerman, S. K., C. T. Noguch, A. N. Schechter, and D. A. Torchia. 1982. Proton enhanced ^{13}C NMR of normal human erythrocytes: characterization of motionally restricted molecules. *Biochem. Biophys. Res. Commum.* 106:1161–1168.
24. Oldfield, E., J. L. Bowers, and J. Forbes. 1987. High-resolution proton and carbon-13 NMR of membranes: why sonicate? *Biochemistry.* 26:6919–6923.
25. Lieber, M. R., Y. Lange, R. S. Weinstein, and T. L. Steck. 1984. Interaction of chlorpromazine with the human erythrocyte membrane. *J. Biol. Chem.* 259:9225–9234.
26. Dodge, J. T., C. Mitchell, and D. J. Hanahan. 1963. The preparation and chemical characteristics of hemoglobin-free ghosts of human erythrocytes. *Arch. Biochem. Biophys.* 100:119–130.
27. Seeman, P. 1972. The membrane actions of anesthetics and tranquilizers. *Pharmacol. Rev.* 24:583–655.
28. Bierboum, T. J., S. R. Bouma, and W. H. Huestis. 1979. A mechanism of erythrocyte lysis by lysophosphatidylcholine. *Biochim. Biophys. Acta.*555:102–110.
29. Seeman, P., W. O. Kwant, and T. Sauks. 1969. Membrane expansion of erythrocyte ghosts by tranquilizers and anesthetics. *Biochim. Biophys. Acta.* 183:499–511.
30. Weltzien, H. U. 1979. Cytolytic and membrane perturbing properties of lysophosphatidylcholine. *Biochim. Biophys. Acta.* 559:259–287.
31. Lange, Y., A. Gough, and T. L. Steck. 1982. Role of bilayer in the shape of the isolated erythrocyte membrane. *J. Membr. Biol.* 69:113–123.
32. McLawhon, R. W., Y. Marikovsky, N. J. Thomas, and R. S. Weinstein. 1987. Ethanol-induced alterations in human erythrocyte shape and surface properties: modulatory role of prostaglandin E_1. *J. Membr. Biol.* 99:73–78.
33. Lepock, J. R., H. E. Frey, H. Bayne, and J. Markus. 1989. Relationship of hyperthermia-induced hemolysis of human eryth-

rocytes to the thermal denaturation of membrane proteins. *Biochim. Biophys. Acta.* 980:191–201.

34. Rand, R. P., W. A. Panglorn, A. D. Purdon, and D. O. Tinker. 1975. Lysolecithin and cholesterol interact stoichiometrically forming bimolecular lamellar structures in the presence of excess water. *Can. J. Biochem.* 53:189–195.

35. Hauser, H., I. Pascher, and S. Sundell. 1980. Conformation of phospholipids: crystal structure of a lysophosphatidylcholine analogue. *J. Mol. Biol.* 137:249–264.

36. Hui, S. W., and C. Huang 1986. X-Ray diffraction evidence for fully interdigitated bilayers of 1-stearoyllysophosphatidylcholine. *Biochemistry.* 25:1330–1335.

37. Saito, H. 1986. Conformation-dependent ^{13}C chemical shift: a new means of conformational characterization as obtained by high-resolution solid-state ^{13}C NMR. *Mag. Res. in Chem.* 24:835–852.

38. Cheney, V. B., and D. M. Grant. 1967. Carbon-13 magnetic resonance. VIII. The theory of carbon-13 chemical shift applied to saturated hydrocarbons. *J. Am. Chem. Soc.* 89:5319–5327.

39. Balchelor, J. G., and J. H. Prestegard. 1972. Conformational analysis of lecithin in vesicles by ^{13}C NMR. *Biochem. Biophys. Res. Commun.* 48:70–75.